*The AAPS Journal, Vol. 13, No. 4, December 2011 (© 2011)*
DOI: 10.1208/s12248-011-9296-3

*Research Article*

*Theme: Pharmacokinetic/Pharmadynamic Modeling and Simulation in Drug Discovery and Translational Research*
*Guest Editors: Cheryl Li, Pratap Singh, and Anjaneya Chimalakonda*

# Quantitative PK–PD Model-Based Translational Pharmacology of a Novel Kappa Opioid Receptor Antagonist Between Rats and Humans

**Cheng Chang,[1,5] Wonkyung Byon,[2] Yifeng Lu,[4] Leslie K. Jacobsen,[4] Lori L. Badura,[4] Aarti Sawant-Basak,[1] Emily Miller,[1] Jing Liu,[3] Sarah Grimwood,[4] Ellen Q. Wang,[2] and Tristan S. Maurer[1]**

*Received 22 April 2011; accepted 1 August 2011; published online 17 August 2011*

***Abstract.*** Pharmacokinetic–pharmacodynamic (PK–PD) modeling greatly enables quantitative implementation of the "learn and confirm" paradigm across different stages of drug discovery and development. This work describes the successful prospective application of this concept in the discovery and early development of a novel κ-opioid receptor (KOR) antagonist, PF-04455242, where PK–PD understanding from preclinical biomarker responses enabled successful prediction of the clinical response in a proof of mechanism study. Preclinical data obtained in rats included time course measures of the KOR antagonist (PF-04455242), a KOR agonist (spiradoline), and a KOR-mediated biomarker response (prolactin secretion) in plasma. Clinical data included time course measures of PF-04455242 and prolactin in 24 healthy volunteers following a spiradoline challenge and single oral doses of PF-04455242 (18 and 30 mg). In both species, PF-04455242 successfully reversed spiradoline-induced prolactin response. A competitive antagonism model was developed and implemented within NONMEM to describe the effect of PF-04455242 on spiradoline-induced prolactin elevation in rats and humans. The PK–PD model-based estimate of $K_i$ for PF-04455242 in rats was 414 ng/mL. Accounting for species differences in unbound fraction, *in vitro* $K_i$ and brain penetration provided a predicted human $K_i$ of 44.4 ng/mL. This prediction was in good agreement with that estimated via the application of the proposed PK–PD model to the clinical data (*i.e.*, 39.2 ng/mL). These results illustrate the utility of the proposed PK–PD model in supporting the quantitative translation of preclinical studies into an accurate clinical expectation. As such, the proposed PK–PD model is useful for supporting the design, selection, and early development of novel KOR antagonists.

**KEY WORDS:** kappa opioid receptor antagonist; PK–PD modeling; proof of mechanism; translational pharmacology.

## INTRODUCTION

As early as 1958, Brodie *et al.* (1) implicated a role for differential half-life and target sensitivity in determining observed species differences in the duration of anesthesia produced by hexobarbitone. Since that time, additional work has been done to support rational cross-species scaling of pharmacokinetics (2–5) and, to a lesser extent, pharmacodynamics (6–10). However, despite knowledge that pharmacological responses differ among species, it remains common practice to select and advance compounds to clinical trials based upon gross pharmacological responses observed in animals. As such, it is perhaps not surprising that safety and efficacy account for most of the unacceptably high rate of attrition currently experienced by the pharmaceutical industry (11,12). This challenge has largely served as the impetus for emerging translational research efforts. A fundamental goal of this effort is to bridge the gap between the "bench" and the "bedside." In other words, at the most basic level, those involved in translational research seek to translate preclinical information into a clinical expectation. One such key expectation in pharmaceutical R&D is a molecule's potential to test a given mechanism of interest in the clinic (*i.e.*, to provide proof of mechanism). This expectation is a critically important driver for decisions regarding chemical optimization, clinical candidate selection, and early clinical trial design. The multidimensional nature of this expectation requires an integrated, multidisciplinary approach (chemistry, biology, pharmacology, ADME, safety, *etc.*). To this end,

Cheng Chang and Wonkyung Byon contributed equally.

[1] Pharmacokinetics, Dynamics and Metabolism, Worldwide Research & Development, Pfizer Inc., Eastern Point Road, Groton, Connecticut, USA.
[2] Clinical Pharmacology, Primary Care Business Unit, Pfizer Inc., Eastern Point Road, Groton, Connecticut, USA.
[3] Clinical Pharmacology, Worldwide Research & Development, Pfizer Inc., Eastern Point Road, Groton, Connecticut, USA.
[4] Neuroscience Research Unit, Worldwide Research & Development, Pfizer Inc., Eastern Point Road, Groton, Connecticut, USA.
[5] To whom correspondence should be addressed. (e-mail: cheng.chang@pfizer.com)

 

pharmacokinetic–pharmacodynamic (PK–PD) modeling is a powerful approach for the systematic integration of diverse preclinical information for the purpose of setting a robust quantitative and unambiguous clinical expectation (13).

In the current work, we describe such an approach that was prospectively taken in the identification and advancement of a novel κ-opioid receptor (KOR) antagonist, PF-04455242 (Fig. 1), for the treatment of depression (14). Proof of mechanism (POM) was assessed via a challenge study which employed the agonist spiradoline (U62,066E). Spiradoline induces elevations in circulating prolactin via direct KOR agonist-mediated inhibition of tuberoinfundibular dopaminergic (TIDA) neurons in the arcuate and median eminence regions of the hypothalamus (15–18). As the TIDA neurons are the major tonic inhibitory regulators of basal prolactin levels (19), reduction in TIDA output results in a subsequent disinhibition of prolactin release from the anterior pituitary. As such, the reduction of spiradoline-induced prolactin increase was selected as the pharmacodynamic marker for characterizing the translational pharmacology of PF-04455242 between rats and humans. In order to facilitate cross-species scaling and comparison, all data were analyzed using a PK–PD model which accounts for spiradoline-induced prolactin release and competitive inhibition of spiradoline by PF-04455242 at the level of the KOR. Overall, the results indicate that clinical POM with PF-04455242 can be predicted from preclinical data using the proposed PK–PD model.

## MATERIALS AND METHODS

### Materials

2-Methyl-*N*-((2′-(pyrrolidin-1-ylsulfonyl)biphenyl-4-yl) methyl)propan-1-amine, hereafter referred to as PF-04455242, and 2-(3,4-dichlorophenyl)-*N*-methyl-*N*-((5S,7R,8R)-7-(pyrrolidin-1-yl)-1-oxaspiro[4.5]decan-8-yl)acetamide, hereafter referred to as spiradoline, were synthesized by the Pfizer Medicinal Chemistry Department (20). Both test compounds were >95% pure, as determined by HPLC. For preclinical studies, test compounds were prepared in sterile water to a dose volume of 2 mL/kg for subcutaneous injection.

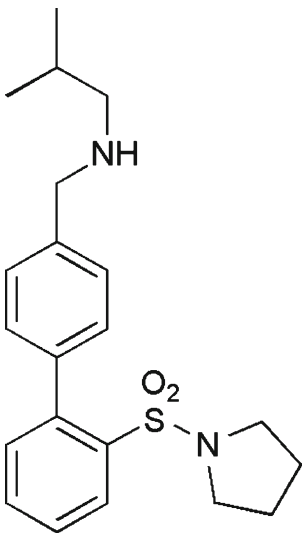


**Fig. 1.** Structure of PF-04455242

For clinical studies, PF-04455242 was prepared as bulk powder for extemporaneous preparation of powder-in-capsule for oral dosing. Spiradoline was prepared as a sterile, clear, colorless solution for intramuscular injection.

### Bioanalytical

#### *Preclinical*

Rat plasma prolactin levels were measured by radioimmunoassay. Aliquots (50 μL) of plasma were analyzed in duplicate with a rat prolactin radioimmunoassay kit (Amersham Biosciences, Piscataway, NJ). The sensitivity of the prolactin assay was 0.07 ng/tube. The intra- and inter-assay coefficients of variation (CV) were 3.2% and 10%, respectively. Each individual kit was calibrated with standard prolactin in the range from 160 pg/tube to 10 ng/tube.

Concentrations of PF-04455242 and spiradoline in rat plasma were determined using a Sciex API model 4000 LC-MS/MS triple quadrupole mass spectrometer. Plasma samples were treated with four times the sample volume of acetonitrile containing a suitable internal standard, centrifuged (4,000×*g*), and 10 μL of clear supernatant was injected into the LC-MS/MS system. Analytes were chromatographically separated followed by data-dependent multiple reaction monitoring (MRM) of ions in a triple quadrupole mass spectrometer. An autosampler was programmed to inject 10 μL on a Phenomenex Synergi Polar-RP 30×2.0 mm 4-μm column using a mobile phase consisting of 0.1% formic acid in 10 mm ammonium formate and acetonitrile at a flow rate of 0.4 mL/min. Ionization was conducted in the positive ion mode at the ionspray interface temperature of 500°C using nitrogen as the nebulizing and heating gas. The ion spray voltage was 4,500 kV. PF-04455242 and spiradoline were analyzed in the MRM mode using the transitions $m/z$ 373→$m/z$ 230 and $m/z$ 425→$m/z$ 354, respectively. Calibration curves were prepared by plotting the appropriate peak area ratios against the concentrations of drug in plasma using $1/x2$ weighting of PF-04455242 or spiradoline/internal standard peak height ratios. The concentration of the analytes in the plasma samples was determined by interpolation from the standard curve, and the dynamic range of the assay was 0.5–2,000 ng/mL.

#### *Clinical*

Healthy volunteer plasma samples were analyzed for PF-04455242 concentrations at Covance Bioanalytical Services, LLC (Indianapolis, USA) using a validated analytical assay in compliance with the sponsor's standard operating procedures. PF-04455242 samples were assayed using a validated, sensitive, and specific high-performance liquid chromatography tandem mass spectrometric method. Calibration standard responses were linear over the range of 0.100–100 ng/mL using a linear regression, 1/concentration. The lower limit of quantification for PF-04455242 was 0.100 ng/mL. Serum prolactin concentrations were measured on a clinical immunoassay analyzer using the Cobas® Prolactin II kit (Roche, USA). The detection method was electrochemiluminescence. The limit of detection was 0.047 μg/L.

### *In Vitro* Studies

KOR binding, $K_i$, was determined using radioligand ([$^3$H]diprenorphine) binding to membranes prepared from Chinese hamster ovary cells expressing either human KOR or rat KOR (14). The unbound fraction of PF-04455242 was determined in rat and human plasma by standard equilibrium dialysis methods (21).

### Preclinical Studies

All procedures were carried out in compliance with the National Institute of Health Guide for the Care and Use of Laboratory Animals (1996) under protocols approved by the Institutional Animal Care and Use Committees. Three independent studies were conducted in rats. In the first study, vehicle (sterile water) or spiradoline (0.1, 0.32, or 1.0 mg/kg, SC) was administered subcutaneously to 300–400 g male Sprague–Dawley rats ($n$=6–9). Blood samples (0.44 mL) were collected from an indwelling jugular vein catheter via a DiLab AccuSampler (North Chelmsford, MA) at 0, 30, 60, and 120 min post-dose for the determination of prolactin concentrations. In a second satellite study, 0.44 mL of blood was collected from rats ($n$=5) for the determination of spiradoline concentrations 30 min post-dose (0.1, 0.32, or 1.0 mg/kg, SC). In a third study, rats ($n$=6–9) were administered vehicle (sterile water) or PF-04455242 (0.32 or 10 mg/kg, SC) 30 min prior to the administration of spiradoline (0.32 mg/kg, SC). Blood samples (0.44 mL) were collected at −30, 10, 20, 30, 45, 60, 90, and 120 min post-spiradoline administration for the determination of prolactin, PF-04455242, and spiradoline concentrations. All blood samples were collected into BD Microtainer tubes (Franklin Lakes, NJ) containing lithium heparin and kept at 4°C. The blood samples were then spun down at 10,000 rpm, 4°C, and plasma was transferred into new tubes and stored at −80°C until analysis as described under bioanalytical methods.

### Clinical Studies

All clinical studies were conducted in compliance with the ethical principles originating in or derived from the Declaration of Helsinki and in compliance with all International Conference on Harmonization Good Clinical Practice Guidelines and the International Ethical Guidelines for Biomedical Research Involving Human Subjects (Council for International Organizations of Medical Sciences 2002). In addition, all local regulatory requirements were followed, in particular those affording greater protection to the safety of study participants. The results from three clinical studies were used to support the analysis: (1) a single dose escalation of PF-04455242 for the initial characterization of population pharmacokinetics in healthy subjects, (2) a multiple-dose escalation of PF-04455242 for the further characterization of population pharmacokinetics in healthy subjects, and (3) a POM study consisting of a spiradoline challenge and two single doses of PF-04455242. In the first study, a single dose of PF-04455242 was administered to 18 healthy subjects for the dose range from 0.5 to 30 mg (22). In a second, multiple-dose study, PF-04455242 was administered to 27 healthy volunteers on an every 6-h basis followed by a single dose on day 7 (23). The third study, POM, consisted of a randomized placebo-controlled parallel group to determine the efficacy of single doses of 18 and 30 mg PF-04455242 in suppressing spiradoline-stimulated serum prolactin secretion relative to placebo in healthy male adult subjects (24). A total of 24 healthy male subjects received a single 18- or 30-mg dose of PF-04455242 or placebo in a 1:1:1 ratio, followed by spiradoline challenge. Subjects received an oral dose of PF-04455242 or placebo at 6 A.M. followed by the administration of 3.2 μg/kg spiradoline intramuscularly (IM) at approximately 7A.M. Blood samples (4 mL) to provide a minimum of 2 mL plasma for PK analysis of PF-04455242 were collected into an appropriately labeled tube containing $K_2$ EDTA before dosing with the study drug and at 15, 30, 45, 60, 75, 90, 105, 120, 135, 150, 165, 180, and 360 min after dosing with the study drug. In addition, blood samples (5 mL) for the measurement of serum prolactin were collected from each subject at screening, before dosing with the study drug, and at 15, 30, 45, 60, 75, 90, 105, 120, 135, 150, 165, and 180 min after dosing with the study drug. Blood for prolactin was collected in a 5-mL serum separator tube (gold cap). All blood samples were centrifuged at approximately 1,700×$g$ for about 10 min at 4°C within 1 h of collection. The plasma was stored in appropriately labeled screw-capped polypropylene tubes at approximately −20°C until analyzed.

### Preclinical PK–PD Modeling

Preclinical PK–PD analysis comprised three steps: (1) the pharmacokinetics of spiradoline were characterized, (2) the pharmacokinetics of PF-04455252 were characterized, and (3) the pharmacodynamics of spiradoline and PF-04455242 were simultaneously characterized while fixing the pharmacokinetic parameters estimated from steps 1 and 2 (Fig. 2). The pharmacokinetics of both spiradoline and PF-04455242 (steps 1 and 2) were characterized using a standard one-compartment model with first-order absorption and elimination. The pharmacodynamic effects of both spiradoline and PF-04455242 were characterized using the model depicted in Eq. 1

$$\mathrm{PRL}_i = \mathrm{BL}_i + \mathrm{STIM}_i, \text{ where } \mathrm{STIM}_i = \frac{E_{\max} \cdot C_{\mathrm{SP},i}^{\gamma}}{\mathrm{EC}_{50}^{\gamma} \cdot \left(1 + \frac{C_{\mathrm{PF},i}}{K_i}\right)^{\gamma} + C_{\mathrm{SP},i}^{\gamma}} \quad (1)$$

where the plasma prolactin level of each individual rat ($\mathrm{PRL_i}$) is a function of that rat's baseline prolactin level ($\mathrm{BL_i}$), plasma spiradoline concentration ($C_{\mathrm{SP,i}}$), and plasma PF-04455242 concentration ($C_{\mathrm{PF,i}}$). $E_{\max}$ and $\mathrm{EC}_{50}$ represent the maximal elevation of prolactin above baseline and the concentration of spiradoline that is associated with half-maximal elevation. $K_i$ represents PF-04455242 *in vivo* potency toward rat KOR, and $\gamma$ is the Hill coefficient describing the steepness of the exposure–response relationship. As such, the proposed model allows for a nonlinear spiradoline concentration-dependent rise in prolactin concentrations above baseline and antagonism by PF-04455242. Consistent with the mechanism of action, the proposed model accounts for antagonist pharmacology via a PF-04455242 concentration-dependent increase in the apparent $\mathrm{EC}_{50}$ of spiradoline.

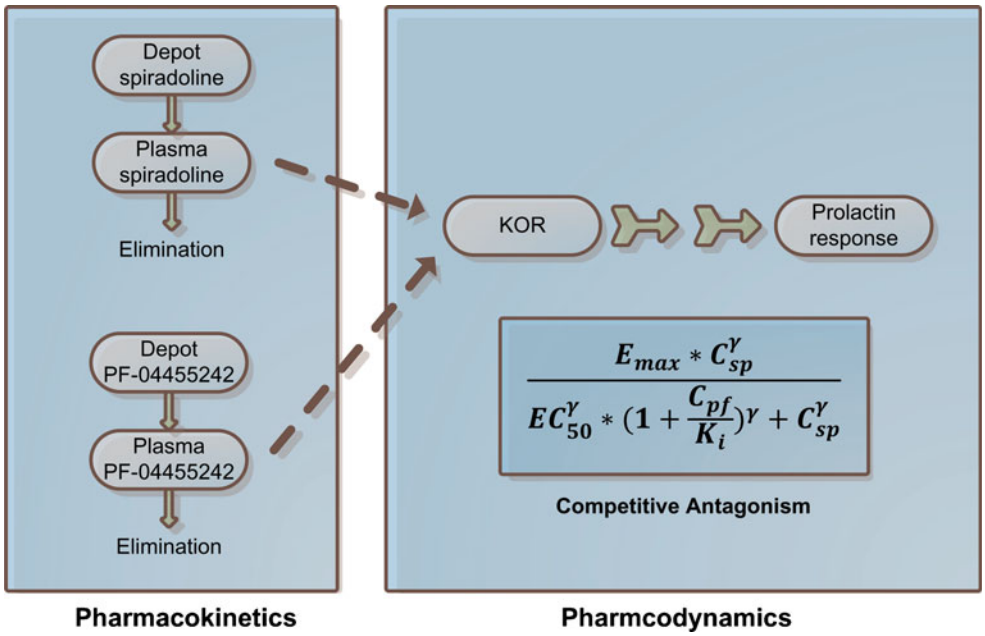


**Fig. 2.** PK–PD model structure. $E_{max}$ is the maximal increase of prolactin under spiradoline stimulation; $C_{sp}$ and $C_{pf}$ represent plasma spiradoline and PF-04455242 concentrations, respectively; $EC_{50}$ represents the concentration of spiradoline that results in half the maximal prolactin increase in the absence of PF-04455242; $K_i$ represents PF-04455242 *in vivo* potency toward rat KOR; and $\gamma$ is the Hill coefficient describing steepness of the exposure–response relationship

## Clinical POM Prediction

The prediction of human PF-04455242 pharmacodynamics in the context of a spiradoline challenge was composed of three components: (1) cross-species scaling of the $K_i$ estimate obtained from the rat PK–PD analysis, (2) prediction of PF-04455242 pharmacokinetics, and (3) accounting for the PK–PD of spiradoline-induced prolactin elevation in a manner that allows for competitive antagonism by PF-04455242. For the first component, cross-species scaling of the $K_i$ parameter was accomplished by accounting for species differences in the unbound plasma fraction and *in vitro* $K_i$ as depicted in Eq. 2

$$K_{i,human,invivo} = K_{i,rat,invivo} \cdot \frac{\mathrm{fu}_{rat}}{\mathrm{fu}_{human}} \cdot \frac{\mathrm{hKOR\_}K_i}{\mathrm{rKOR\_}K_i} \tag{2}$$

where $\mathrm{fu}_{rat}$ and $\mathrm{fu}_{human}$ parameters represent the unbound fraction of PF-04455242 determined via an independent equilibrium dialysis study for human and rat plasma, respectively, and hKOR_$K_i$ and rKOR_$K_i$ are the $K_i$ values of PF-04455242 determined via an independent *in vitro* competitive binding assay for the human and rat KOR, respectively. Inclusion of the *in vitro* receptor binding potency correction is based on a previous observation from several drugs where relative receptor binding affinity has been shown to correlate with the *in vivo* estimate of drug potency (25–28). For the second component, human plasma exposures of PF-04455242 were simulated using a population pharmacokinetic model derived from pharmacokinetic studies in healthy subjects (described in "Clinical PK–PD Model" below). This enabled a focused examination of the translational pharmacology without the potentially confounding influence of errors in pharmacokinetic predictions based on preclinical data. For the third component, data illustrating the relationship between spiradoline administration and prolactin elevation in humans were extracted from the literature (17,18). Although the pharmacokinetics of spiradoline in humans were not measured, the results of these studies indicate that the prolactin response is dose-linear over the range of reported doses (1.6–4 μg/kg). In particular, it was apparent that a twofold increase in an intramuscular dose of spiradoline from 1.6 to 3.2 μg/kg produced a mean twofold increase in prolactin elevation above baseline (17). Similarly, from a separate study, a 2.5-fold increase of spiradoline dose from 1.6 to 4 μg/kg resulted in a mean 2.3-fold increase of prolactin elevation above baseline (18). Together with an assumption of linear pharmacokinetics, these observations enabled the modification of Eq. 1 such that measurements of spiradoline concentration, $E_{max}$ and $EC_{50}$, become unnecessary in predicting clinical POM outcome. In the first step, we assume that spiradoline-mediated elevation in human plasma prolactin (above baseline) follows a sigmoid $E_{max}$ model as described above for rats (Eq. 3).

$$\mathrm{STIM} = \frac{E_{max} \cdot C_{SP}^{\gamma}}{EC_{50}^{\gamma} + C_{SP}^{\gamma}} \tag{3}$$

Assuming that an $x$-fold increase in plasma spiradoline concentration ($C_{sp}$) produces the same $x$-fold elevation in plasma prolactin concentration (PRL), one obtains Eq. 4.

$$x \cdot \mathrm{STIM} = \frac{E_{max} \cdot (x \cdot C_{SP})^{\gamma}}{EC_{50}^{\gamma} + (x \cdot C_{SP})^{\gamma}} \tag{4}$$

Substituting Eq. 3, one obtains Eq. 5.

$$x \cdot \frac{E_{max} \cdot (C_{SP})^{\gamma}}{EC_{50}^{\gamma} + (C_{SP})^{\gamma}} = \frac{E_{max} \cdot (x \cdot C_{SP})^{\gamma}}{EC_{50}^{\gamma} + (x \cdot C_{SP})^{\gamma}} \tag{5}$$

Simplifying in order to define $(x \cdot C_{sp})^{\gamma}$ in terms of $EC_{50}{}^{\gamma}$, one obtains Eq. 6.

$$C_{SP}^{\gamma} = a \cdot EC_{50}^{\gamma}, \text{where } a = \frac{1 - x^{1-\gamma}}{x - 1} \tag{6}$$

Consequently, the relationship between $x$-fold of $C_{sp}$ and $EC_{50}{}^{\gamma}$ could be expressed as:

$$(x \cdot C_{SP})^{\gamma} = a \cdot x^{\gamma} \cdot EC_{50}^{\gamma}, \text{where } a = \frac{1 - x^{1-\gamma}}{x - 1} \tag{7}$$

Substituting Eq. 7 into the STIM function in Eq. 1 and simplifying, one obtains Eq. 8 to describe the stimulation effect at $x$-fold of $C_{sp}$.

$$\text{STIM} = \frac{E_{max} \cdot x^{\gamma} \cdot a}{\left(1 + \frac{C_{PF}}{K_i}\right)^{\gamma} + x^{\gamma} \cdot a} \tag{8}$$

This enables the removal of both the $C_{sp}$ and $EC_{50}$ terms associated with spiradoline from the PK–PD model, leaving only the $E_{max}$ and $\gamma$ terms. Expressing stimulation as a fraction of that in the uninhibited state and simplifying enables removal of the $E_{max}$.

$$\frac{\text{STIM}_{\text{inhibited}}}{\text{STIM}_{\text{uninhibited}}} = \frac{1 + x^{\gamma} \cdot a}{\left(1 + \frac{C_{PF}}{K_i}\right)^{\gamma} + x^{\gamma} \cdot a} \tag{9}$$

Expanding Eq. 9 according to Eq. 6 and simplifying, one obtains Eq. 10.

$$\frac{\text{STIM}_{\text{inhibited}}}{\text{STIM}_{\text{uninhibited}}} = \frac{x^{\gamma} - 1}{(x - 1) \cdot \left(1 + \frac{C_{PF}}{K_i}\right)^{\gamma} + x^{\gamma} - x} \tag{10}$$

The final form of the model used to predict the effect of PF-04455242 on spiradoline-induced prolactin elevation in humans is depicted in Eq. 11.

$$PRL = BL + \text{STIM}_{\text{placebo}} \cdot \frac{x^{\gamma} - 1}{(x - 1) \cdot \left(1 + \frac{C_{PF}}{K_i}\right)^{\gamma} + x^{\gamma} - x} \tag{11}$$

where $\text{STIM}_{\text{placebo}}$ represents the observed spiradoline-induced prolactin elevation above baseline in healthy subjects receiving placebo. $\text{STIM}_{\text{placebo}}$ and BL were obtained via the digitization of the reported prolactin response following IM administration of 4 μg/kg spiradoline (18) and subsequent linear scaling to the 3.2 μg/kg spiradoline dose used in the current clinical POM study design. As mentioned above, an approximately twofold proportionality between prolactin response and spiradoline in the dose range from 1.6 to 4 μg/kg was observed from two clinical studies (17,18), and thus $x$ was set to 2 in Eq. 11. Lastly, the $\gamma$ parameter was assumed to be 4.15, consistent with that estimated in rats.

## Clinical PK–PD Model

A sequential PK–PD analysis was performed by first developing a population PK model and then applying the proposed PK–PD model (Eq. 11) to describe the relationship between PF-04455242 concentration and inhibition of spiradoline-stimulated serum prolactin increase from the clinical POM study. A total of 943 PF-04455242 concentrations were available from single- (22) and multiple-dose PK studies (23) in healthy volunteers. A standard two-compartment model with zero-order absorption and first-order elimination was used to characterize these data. Using the population PK model developed from single- and multiple-dose PK studies, the individual maximum a posteriori Bayesian estimate of PF-04455242 PK parameters were estimated based on the observed PF-04455242 concentrations for each subject in the clinical POM study. Individual concentrations were predicted using these individual parameters and combined with the serum prolactin data to generate the time-matched PF-04455242 concentration and prolactin dataset. The direct response competitive antagonism model developed from preclinical experiments (Eq. 11) was adapted to the clinical POM data by modifying the $\text{STIM}_{\text{placebo}}$ function, which was empirically modeled using a Weibull function as shown in Eq. 12:

$$\text{STIM}_{\text{placebo}} = BL \cdot \frac{\kappa}{\lambda} \left(\frac{\text{TIME}}{\lambda}\right)^{\kappa - 1} \cdot \exp^{-(\text{TIME}/\lambda)^{\kappa}} \tag{12}$$

where BL is the baseline prolactin level in healthy volunteers, $\kappa$ is the shape parameter, $\lambda$ is the scale parameter of the distribution, and TIME is the time in hours after spiradoline administration. Inter-individual variance (IIV) terms in the

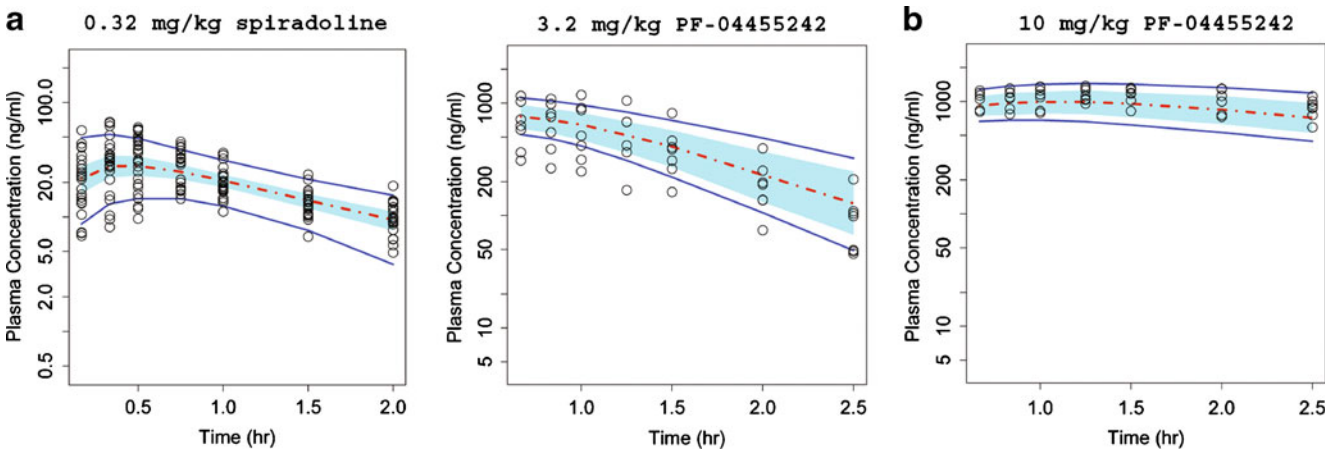


**Fig. 3.** Comparison of model-simulated time courses of spiradoline concentration (**a**) and PF-04455242 concentration (**b**) to observations in rats. *Open circles* represent observed data, *dashed red line* represents the simulated median, and *solid blue lines* represent the mean 5th and 95th percentiles from the simulated trials. The *blue band around the solid red line* represents 90% prediction interval of the simulated median

**Table I.** Pharmacokinetic Parameter Estimates for Spiradoline and PF-04455242 in Rats

| Compound | Parameter | Estimate | CV (%) |
|---|---|---|---|
| Spiradoline | CL/F (L $h^{-1}$ $kg^{-1}$) | 6.06 | 5.08 |
| | Vc/F (L/kg) | 7.15 | 8.84 |
| | Ka ($h^{-1}$) | 4.75 | 14.25 |
| | $\omega_{CL}$ (%) | 18.0 | 49.8 |
| | $\omega_{VC}$ (%) | 46.5 | 22.6 |
| | $\omega_{Ka}$ (%) | 59.1 | 50.4 |
| | Proportional error (%) | 44.72 | 43.2 |
| PF-04455242 | CL/F (L $h^{-1}$ $kg^{-1}$) | 2.5 | 12.6 |
| | Vc/F (L/kg) | 1.31 | 20.4 |
| | Ka ($h^{-1}$) | 1.64[a]/0.385[b] | 11.0[a]/16.8[b] |
| | $\omega_{CL}$ (%) | 35.6 | 43.7 |
| | $\omega_{VC}$ (%) | 26.1 | 85.2 |
| | $\omega_{Ka}$ (%) | 31.9[a]/NE[b] | 45.4[a]/NE[b] |
| | Proportional error (%) | 14.1 | 24.8 |

*NE* not estimated
[a] Parameter estimate for 3.2 mg/kg
[b] Parameter estimate for 10 mg/kg

PK–PD model were chosen from an additive model or an exponential error model as appropriate.

## Data Analysis

The PK–PD data were modeled using nonlinear mixed-effects modeling as implemented in the NONMEM (NONMEM software system, version VI, GloboMax LLC, Hanover, MD) (29). Both preclinical and clinical analyses were conducted using the first-order conditional estimation with interaction (FOCE INTERACTION) method. Graphical data display was done using either R.2.11.1 or S-PLUS (version 8.0, Insightful). Both preclinical and clinical population PK analyses were focused on developing a structural pharmacokinetic model without covariates. The IIV terms in the population PK model were described by an exponential error model (Eq. 13), where $P_i$ is the estimated pharmacokinetic parameter value for individual $i$, $\widehat{P}$ is the population mean value of the parameter, and $\eta^{Pi}$ is the individual-specific inter-individual random effects of parameter $P$ for individual $i$, which are assumed to be symmetrically and independently distributed with mean 0 and variance $\omega^2$: $\eta \sim N(0, \omega^2)$ with covariance defined by the inter-individual covariance matrix. An attempt was made to define a block covariance matrix for the inter-individual random effects ($\eta$) between CL/F and Vc/F.

$$P_i = \widehat{P}\exp(\eta^{Pi}) \tag{13}$$

Since a log transform-both-sides approach was used in the clinical population PK model, the residual error model was described by Eq. 14, where $C_{ij}$ is the $j$th plasma concentration measured in the $i$th individual, $\hat{C}_{ij}$ is the individual model-predicted plasma concentration, and $\varepsilon_{ij}$, is the proportional component:

$$Ln(C_{ij}) = Ln\left(\widehat{C}_{ij}\right) + \varepsilon_{ij} \tag{14}$$

## Assessment of the Model Goodness of Fit

Assessment of the model goodness of fit was conducted based on standard methods (29,30). Models were evaluated using the following goodness-of-fit criteria: successful mini-

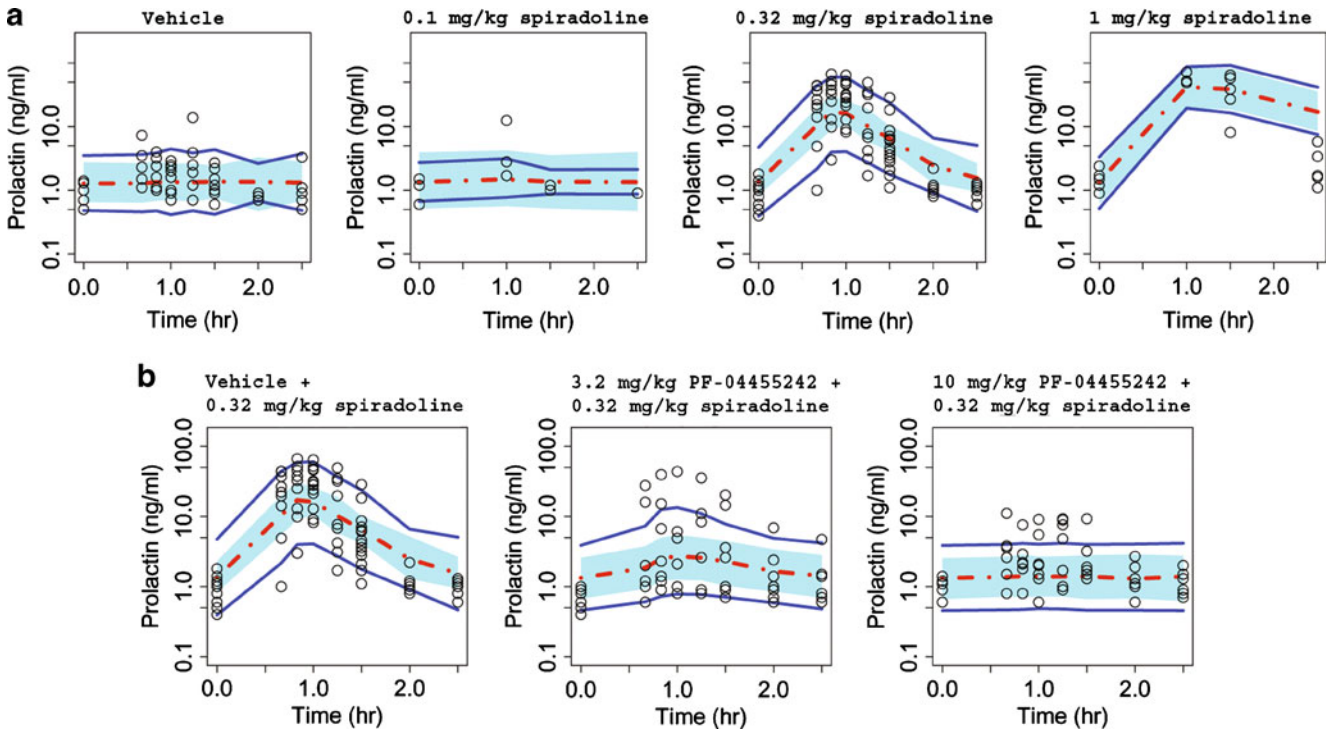


**Fig. 4.** Comparison of model-simulated time courses of rat prolactin concentrations from spiradoline dose–response study (**a**) and PF-04455242 dose–response study (**b**) to observations. *Open circles* represent observed data, *dashed red line* represents the simulated median, and *solid blue lines* represent the mean 5th and 95th percentiles from the simulated trials. The *blue band around the solid red line* represents 90% prediction interval of the simulated median

**Table II.** Pharmacodynamic Parameter Estimates for Prolactin Response in Rats

| Parameter | Estimate | CV (%) |
|---|---|---|
| Baseline PRL (ng/mL) | 1.34 | 8.58 |
| $E_{max}$ (ng/mL) | 39.7 | 29.0 |
| $EC_{50}$ (ng/mL) | 34.3 | 25.1 |
| $K_i$ (ng/mL) | 414 | 31.4 |
| $K_{i,unbound}$ (nM) | 33 | – |
| $\gamma$ | 4.15 | 25.1 |
| $\omega_{BL}$ (%) | 39.1 | 37.4 |
| Proportional error (%) | 131 | 7.31 |

mization of the objective function; visual inspection of several diagnostic scatter plots (population and individual observed *versus* predicted concentrations, residual plots, plots of random effects, and weighted residuals *versus* time, histograms of individual random effects); change in the objective function value (OFV) relative to the change in number of parameters; the magnitude and precision of the parameter estimates; as well as changes in both inter-individual and residual variability. NONMEM OFV is proportional to −2 times the log-likelihood, given a vector of parameter estimates. If two models were nested, the difference in OFV (ΔOFV) was calculated and the reduction of 3.84 was considered statistically significant ($P<0.05$) at the degree of freedom (*df*) of 1 since ΔOFV approximately follows $\chi^2$ distribution. All parameter estimates were reported with a measure of estimation uncertainty, such as the standard error of the estimates (obtained from the NONMEM $COVARIANCE step).

### Assessment of Model Predictive Performance (Validation)

As described in the FDA's Guidance for Industry: Population Pharmacokinetics (30), the objective of model evaluation was to examine whether the model provided a good description of the data in terms of its behavior and of the application proposed. The adequacy of the final model and parameter estimates was investigated with a visual predictive check (VPC) method. This is similar to the posterior predictive check, but assumes that parameter uncertainty is negligible, relative to inter-individual and residual variance (31). The basic premise is that a model and the parameters derived from an observed dataset should produce simulated data that are similar to the original observed data. Any problems evident in the simulations were investigated and further model development was conducted as necessary.

## RESULTS

### *In Vitro* Studies

The unbound fraction of PF-04455242 was estimated to be similar between human and rat plasma (0.04 and 0.03, respectively). In contrast, the *in vitro* $K_i$ estimate of PF-04455242 for the human KOR was substantially lower (more potent) than that obtained for the rat KOR (3 *versus* 21 nM, respectively) (14).

### Preclinical PK–PD

Rat plasma concentration–time profiles for both spiradoline and PF-04455242 were well described by a one-compartment model with first-order absorption and elimination (Fig. 3). Spiradoline pharmacokinetics were characterized by a single set of population mean parameter estimates, while the description of PF-04455242 pharmacokinetics required a dose-dependent absorption rate constant (Table I). After subcutaneous dosing, spiradoline was rapidly absorbed, while PF-04455242 absorption was relatively slower and dose-dependent. At 10 mg/kg, PF-04455242 absorption lasted throughout the pharmacodynamic measurement time period (0–2.5 h).

The proposed PK–PD model well characterized the pharmacodynamics of spiradoline-induced prolactin secretion and antagonism by PF-04455242, where the VPC plot shows that most of the observed prolactin responses fall within the 90% prediction interval (Fig. 4). The model results (Table II) indicate that spiradoline produces a nonlinear, concentration-dependent increase in plasma prolactin to a maximum of 39.7 ng/mL above a baseline of 1.34 ng/mL. The concentration dependence was characterized by a spiradoline $EC_{50}$

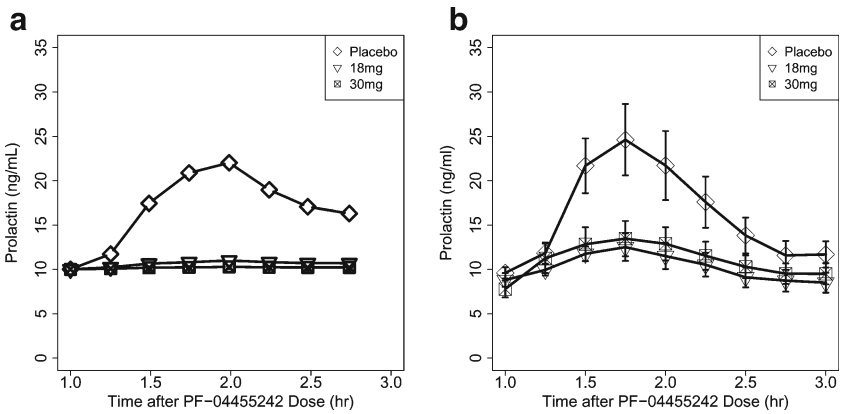


**Fig. 5.** Predicted prolactin response in healthy volunteers based on preclinical PK–PD model (**a**) and observed prolactin response in healthy volunteers (**b**), where data shown are the mean ± SEM ($n=8$ healthy volunteers per treatment group)

**Table III.** Pharmacokinetic Parameter Estimates for PF-04455242 in Healthy Volunteers

| Parameter | Estimate | CV (%) |
|---|---|---|
| CL/F (L/h) | 54.6 | 8.55 |
| Vc/F (L) | 327 | 7.00 |
| Duration (h) | 1.24 | 6.14 |
| Vp/F (L) | 58.5 | 17.3 |
| Q/F(L/h) | 6.51 | 28.1 |
| Alag (hr) | 0.374 | 5.59 |
| $\omega_{CL}$ (%) | 53.7 | 20.3 |
| $\omega_{VC}$ (%) | 48.5 | 20.2 |
| cov($\omega_{CL}$, $\omega_{VC}$) | 48.5 | 21.3 |
| $\omega_{D1}$ (%) | 30.6 | 34.9 |
| $\omega_{VP}$ (%) | 27.3 | 38.0 |
| $\omega_{Q}$ (%) | 27.3 | 38.0 |
| $\omega_{ALAG1}$ (%) | 26.6 | 53.0 |
| Proportional error (%) | 32.6 | 8.16 |

and $\gamma$ of 34.3 ng/mL and 4.15, respectively. PF-04455242 substantially inhibited spiradoline-induced prolactin response at both doses tested (3.2 and 10 mg/kg). The concentration dependence of this antagonist response was characterized by a PF-04455242 $K_i$ estimate of 414 ng/mL (33 nM, unbound). Although the preclinical prolactin assay was highly variable (estimated residual variability of 131%), robust response still supported a precise identification of the pharmacodynamic parameters in rats (Table II).

### Clinical POM Prediction

Correcting for species differences in the unbound fraction and *in vitro* $K_i$, according to Eq. 2, provided a PF-04455242 human $K_i$ prediction of 44.4 ng/mL (4.8 nM, unbound). Combining this with exposure predictions from the human population PK model in the context of Eq. 10 provided a prediction that the 18- and 30-mg doses of PF-04455242 would substantially suppress spiradoline-induced prolactin elevation in humans (Fig. 5a). This prediction of PF-04455242 response was consistent with that observed in the clinical trial (Fig. 5b).

### Clinical PK–PD

Final parameter estimates from the population PK model are summarized in Table III, and only the VPC results for the single 18- and 30-mg doses employed in the spiradoline challenge study are shown in Fig. 6. As with the preclinical model, the clinical VPC results show that most of the observed plasma concentrations fall within the 90% prediction interval, indicating that the final model adequately described the PF-04455242 concentration–time profile. In the POM study, a reduction of spiradoline (3.2 μg/kg, IM)-stimulated serum prolactin increase by PF-04455242 (both 18 and 30 mg, PO) was observed (Fig. 5b). The time-matched PF-04455242 concentration and prolactin data were modeled using Eqs. 11 and 12, and the final parameter estimates are summarized in Table IV. The human $K_i$ was estimated to be 39.2 ng/mL (4.2 nM, unbound) with a $\gamma$ estimate of 1.66. The VPC results (Fig. 7) show that most of the observed prolactin responses fell within the 90% prediction interval, indicating that the final model adequately describes the relationship between PF-04455242 concentration and inhibition of spiradoline-stimulated serum prolactin. Other than the Hill coefficient $\gamma$ (CV of 79.3%) from the clinical model, structural parameters from both the preclinical and clinical models were sufficiently estimated, as indicated by relatively small CVs (Tables I, II, III, and IV). Although prolactin baseline levels were estimated to be different between rats and humans (1.34 and 9.53 ng/mL, respectively), the inter-individual variability of prolactin baseline levels in both species were quite comparable (39% and 33% for rats and humans, respectively).

## DISCUSSION

### Preclinical PK–PD and Clinical POM Prediction

Spiradoline is known to induce an increase in plasma prolactin concentration through its agonist activity at the KOR. In addition, the pharmacology and safety of spiradoline has been studied previously in both rats and humans. As such, antagonism of the prolactin response to a spiradoline challenge represents a safe and convenient means of providing

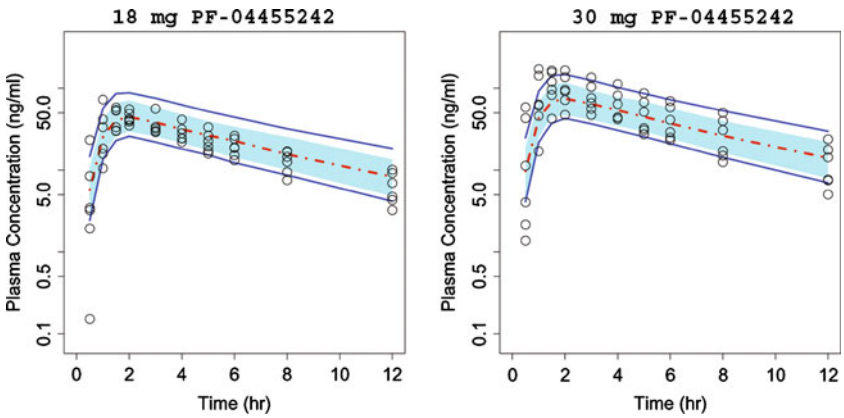


**Fig. 6.** Comparison of model-simulated time courses of PF-04455242 concentration in healthy volunteers to observations. *Open circles* represent observed data, *dashed red line* represents the simulated median, and *solid blue lines* represent the mean 5th and 95th percentiles from the simulated trials. The *blue band around the solid red line* represents 90% prediction interval of the simulated median

**Table IV.** Pharmacodynamic Parameter Estimates for Prolactin Response in Healthy Volunteers

| Parameter | Estimate | CV (%) |
|---|---|---|
| Baseline PRL (ng/mL) | 9.53 | 6.89 |
| Kappa | 2.49 | 8.31 |
| Lambda | 0.943 | 5.78 |
| $K_i$ (ng/mL) | 39.2 | 33.4 |
| $K_{i,\text{unbound}}$ (nM) | 4.2 | |
| $\gamma$ | 1.5 | 79.3 |
| $\omega_{BL}$ (ng/mL) | 3.1 | 23.7 |
| $\omega_{\text{Lambda}}$ (%) | 19.9 | 79.8 |
| Proportional error (%) | 17.5 | 12.7 |

POM for PF-04455242. Accordingly, the preclinical PK–PD characterization of PF-04455242 described herein employed a spiradoline challenge model such that the results could be scaled to support the design of a comparable human POM study. Preclinically, the proposed competitive interaction PK–PD model adequately characterized the effect of both spiradoline and PF-04455242 on plasma prolactin concentration in rats (Figs. 3 and 4). The lack of a time dependency in the concentration–effect relationship of both spiradoline and PF-04455242 within the model is generally consistent with the rapid signal transduction and turnover of endogenous prolactin (32,33). The estimated model parameters indicate that plasma prolactin concentrations increase steeply with spiradoline concentration ($\gamma$=4.15), reaching a maximum elevation of approximately 30-fold higher than baseline levels (baseline=1.34 ng/mL, $E_{max}$=39.7 ng/mL). This finding is generally consistent with that observed in monkeys where plasma prolactin concentrations have been shown to increase steeply with spiradoline dose to a maximum elevation of approximately 20-fold baseline levels (16). Competitive antagonism of this response by PF-04455242 in rats is characterized by an estimated $K_i$ value of 414 ng/mL (33 nM, unbound). This estimate is consistent with that estimated for rat KOR *in vitro* (21 nM). These findings suggest that the PK–PD model described in Eq. 1 provides a reasonable framework from which to rationally scale *in vitro* and *in vivo* pharmacology data generated preclinically.

Unfortunately, the lack of human pharmacokinetic data for spiradoline precluded the direct application of Eq. 1 to support human pharmacodynamic predictions. In addition, although the analgesic effects of spiradoline have been extensively studied in humans, an examination of the complete dose–response for prolactin elevation has been precluded by side effects such as diuresis, sedation, and dysphoria (17,18,34,35). As such, the stimulation portion of Eq. 1 was redefined based upon the observation that placebo-corrected prolactin concentrations increase approximately twofold between spiradoline doses of 1.6 and 3.2 μg/kg (17). Assuming further that this twofold change in dose confers a twofold difference in concentration enabled the definition of spiradoline concentration as a function of $EC_{50}$ (Eq. 6). Finally, redefining the stimulation function as a fraction of the uninhibited state provided a human PK–PD model that was analogous to that used in the characterization of rat PK–PD without requiring information regarding spiradoline concentration, $EC_{50}$, or $E_{max}$ (Eq. 11). The only remaining parameter of direct relevance to spiradoline pharmacodynamics is the unitless $\gamma$, which, in the absence of further information, was simply assumed to translate 1:1 between rats and humans. With this simplification, only parameters defining expected PF-04455242 plasma exposure and KOR inhibitory potency were required to support human POM predictions.

In the current exercise, human PF-04455242 exposures were simulated using a population pharmacokinetic model derived from phase I results. In practice, the use of phase I pharmacokinetic data in this manner would be most useful in a POM study design as it would be expected to provide the most accurate prediction of human exposure. An alternative approach, which is not described here, is to use available methods for predicting human pharmacokinetics from preclinical data. As a variety of such methods have been shown to provide predictions of reasonable accuracy, this approach would be warranted at earlier stages of research to support drug design and clinical candidate selection. For the final component of the human POM prediction, the expected inhibitory potency of PF-04455242 was obtained via scaling of the estimate obtained in rats using Eq. 2, which accounts for species differences in unbound plasma fraction and *in vitro* KOR potency. Accordingly, the $K_i$ estimate of 414 ng/mL (33 nM, unbound) obtained in rats was scaled to an expected value of 44.4 ng/mL (4.8 nM, unbound) in humans. In this particular case, the difference in expected potency between

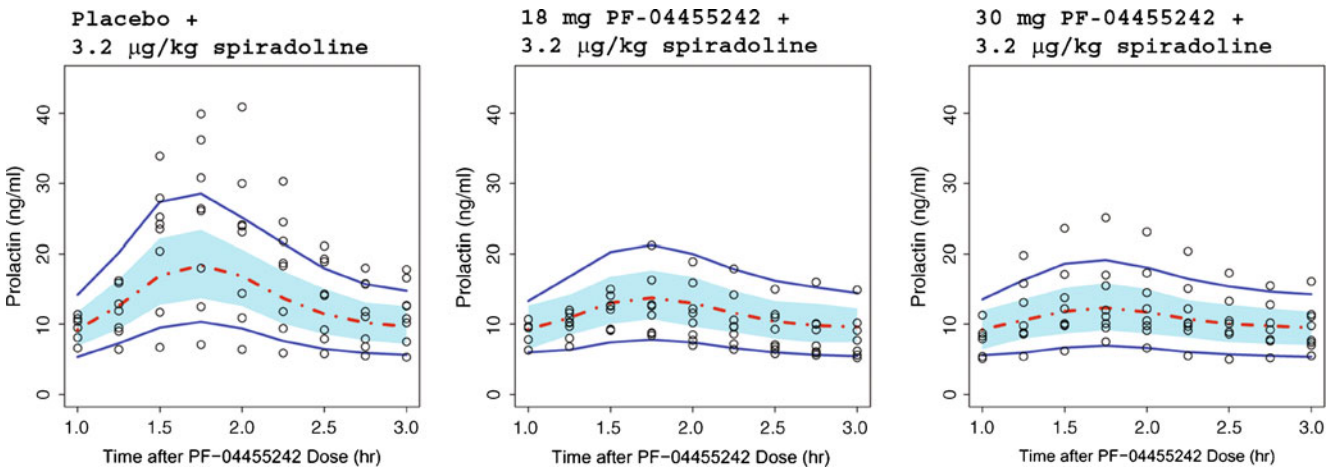


**Fig. 7.** Comparison of model-simulated time courses of prolactin concentrations in healthy volunteers to observed data in the clinical POM study. *Open circles* represent observed data, *dashed red line* represents the simulated median, and *solid blue lines* represent the mean 5th and 95th percentiles from the simulated trials. The *blue band around the solid red line* represents 90% prediction interval of the simulated median

species was primarily driven by that observed against rat and human KOR *in vitro* (3 and 21 nM, respectively). An alternative approach to predicting human potency would be to use the *in vitro* $K_i$ estimate obtained against human KOR directly. This approach is supported by the concordance of *in vitro* and *in vivo* $K_i$ estimates obtained in rats (21 *versus* 33 nM, respectively). Such an approach would be particularly useful in providing context to *in vitro* assays which drive drug design in the earliest stages of research. Lastly, it is important to note that accounting for species differences in the rate and extent of distribution to the target tissue may also be required in some cases. This may be of particular importance in cases, like KOR, where the target lies behind the blood–brain barrier. However, in the current case, species differences in distribution to the brain were assumed to be negligible based on preclinical studies that indicated a rapid 1:1 equilibration of PF-04455242 across the blood–brain barrier (data not shown).

With these assumptions and scaling exercises in place, the model was used to predict that both the 18- and 30-mg doses of PF-04455242 would produce a near-complete suppression of spiradoline-induced prolactin secretion in the human POM study. These predictions were generally consistent with clinical observations (Fig. 5). As such, these results support the utility of the proposed model, scaling methods and simplifying assumptions in supporting POM predictions of sufficient accuracy to aid decision making (*e.g.*, compound design, candidate selection, and POM trial design).

### Clinical PK–PD

Although the proposed model combining clinical PK parameters and projected PD parameters based on preclinical results successfully predicted the general behavior of PF-04455242 in the clinical POM trial (Fig. 5), careful inspection revealed an over-prediction in the degree of prolactin suppression at both dose levels. This result could be related to either an under-prediction of PF-04455242 *in vivo* $K_i$ or over-prediction of $\gamma$ during the translational exercise. As such, these parameters were directly estimated from the application of the reduced form of the PK–PD model (Eq. 11) to the observed clinical data.

The results of this exercise indicated that the estimated $K_i$ value (39 ng/mL, 4.2 nM, unbound) was quite consistent with that predicted from the preclinical analysis (44 ng/mL, 4.8 nM, unbound). In addition, these estimates are both very similar to that estimated against human KOR *in vitro* (3 nM). These findings clearly demonstrate that the $K_i$ of PF-04455242 scales well with relative binding affinities to KOR determined *in vitro*. Although full-length rat and human KOR share 94% homology, their antagonist binding sites are more variable (91% homology), contributing to the sevenfold binding potency difference for PF-04455242. For this reason, it is highly desirable to determine the relative *in vitro* potency of compounds against the target of interest across species and explicitly account for such differences within the proposed PK–PD model. For example, in the absence of guidance from *in vitro* binding results, PF-04455242 would not have been advanced to the clinic because the model-based prolactin response prediction would have been too small to be detectable. Furthermore, the current analysis indicates an excellent concordance between the model-based $K_i$ estimate and that obtained *in vitro* in both rats and humans. Overall, these findings support previous assertions that *in vivo* potency estimates derived from preclinical PK–PD modeling are more likely to translate between biological systems (36). As such, it is highly desirable to develop these models at the earliest stages of pharmaceutical research so as to provide context to the *in vitro* pharmacology data which drive the drug design process. This will help ensure that only molecules capable of safely and effectively testing the mechanism of interest are advanced to clinical trials.

In contrast to $K_i$, the $\gamma$ parameter was found to be different between rats and humans (4.15, *versus* 1.5, respectively). This finding suggests that the relationship between spiradoline concentration and prolactin effect is steeper in rats than in humans. As this parameter is purely empirical in nature, it is not possible to provide an explanation for this species difference at this time. Nevertheless, in this case, the clinical POM predictions were of sufficient accuracy to ensure a reasonable POM result despite the inability to accurately scale this particular parameter.

## CONCLUSION

This work illustrates how a PK–PD model was used to facilitate the quantitative translation of preclinical pharmacology data on KOR antagonism to the clinic in support of POM. The application of such approaches is expected to increase the rate of success in the clinic by ensuring the identification of POM-ready molecules and the rational design of such studies. Although the described application is specific to the novel KOR antagonist, PF-04455242, the underlying principles and assumptions employed are generally relevant to translational pharmacology efforts.

## ACKNOWLEDGMENTS

The authors would like to thank Hugh Barton, Adam Ogden, Ken Kowalski, and Yasong Lu for insightful discussions on the work described herein.

## REFERENCES

1. Quinn GP, Axelrod J, Brodie BB. Species, strain and sex differences in metabolism of hexobarbitone, amidopyrine, antipyrine and aniline. Biochem Pharmacol. 1958;1:152–9.
2. Boxenbaum H. Interspecies scaling, allometry, physiological time, and the ground plan of pharmacokinetics. J Pharmacokinet Biopharm. 1982;10(2):201–27.
3. Rane A, Wilkinson GR, Shand DG. Prediction of hepatic extraction ratio from *in vitro* measurement of intrinsic clearance. J Pharmacol Exp Ther. 1977;200(2):420–4.
4. Nestorov I. Whole-body physiologically based pharmacokinetic models. Expert Opin Drug Metab Toxicol. 2007;3(2):235–49.
5. Hosea NA, Collard WT, Cole S, Maurer TS, Fang RX, Jones H, *et al*. Prediction of human pharmacokinetics from preclinical information: comparative accuracy of quantitative prediction approaches. J Clin Pharmacol. 2009;49(5):513–33.
6. Mager DE, Jusko WJ. Development of translational pharmacokinetic–pharmacodynamic models. Clin Pharmacol Ther. 2008;83(6):909–12.
7. Mager DE, Woo S, Jusko WJ. Scaling pharmacodynamics from *in vitro* and preclinical animal studies to humans. Drug Metab Pharmacokinet. 2009;24(1):16–24.

8. Lepist EI, Jusko WJ. Modeling and allometric scaling of s(+)-ketoprofen pharmacokinetics and pharmacodynamics: a retrospective analysis. J Vet Pharmacol Ther. 2004;27(4):211–8.
9. Woo S, Jusko WJ. Interspecies comparisons of pharmacokinetics and pharmacodynamics of recombinant human erythropoietin. Drug Metab Dispos. 2007;35(9):1672–8.
10. Zuideveld KP, Van der Graaf PH, Peletier LA, Danhof M. Allometric scaling of pharmacodynamic responses: application to 5-Ht1A receptor mediated responses from rat to man. Pharm Res. 2007;24(11):2031–9.
11. Lindner MD. Clinical attrition due to biased preclinical assessments of potential efficacy. Pharmacol Ther. 2007;115(1):148–75.
12. Schuster D, Laggner C, Langer T. Why drugs fail—a study on side effects in new chemical entities. Curr Pharm Des. 2005;11 (27):3545–59.
13. Danhof M, de Lange EC, Della Pasqua OE, Ploeger BA, Voskuyl RA. Mechanism-based pharmacokinetic–pharmacodynamic (PK–PD) modeling in translational drug research. Trends Pharmacol Sci. 2008;29(4):186–91.
14. Grimwood S, Lu Y, Schmidt AW, Vanase-Frawley MA, Sawant-Basak A, Miller E, McLean S, Freeman J, Wong S, McLaughlin JP, Verhoest PR. Pharmacological characterization of 2-methyl-N-((2'-(pyrrolidin-1-ylsulfonyl)biphenyl-4-yl)methyl)propan-1-amine (PF-04455242), a high-affinity antagonist selective for kappa opioid receptors. J Pharmacol Exp Ther. 2011. doi:10.1124/jpet.111.185108.
15. Di Chiara G, Imperato A. Opposite effects of mu and kappa opiate agonists on dopamine release in the nucleus accumbens and in the dorsal caudate of freely moving rats. J Pharmacol Exp Ther. 1988;244(3):1067–80.
16. Butelman ER, Harris TJ, Kreek MJ. Effects of E-2078, a stable dynorphin A(1–8) analog, on sedation and serum prolactin levels in rhesus monkeys. Psychopharmacology (Berl). 1999;147(1):73–80.
17. Chappell PB, Leckman JF, Scahill LD, Hardin MT, Anderson G, Cohen DJ. Neuroendocrine and behavioral effects of the selective kappa agonist spiradoline in Tourette's syndrome: a pilot study. Psychiatry Res. 1993;47(3):267–80.
18. Ur E, Wright DM, Bouloux PM, Grossman A. The effects of spiradoline (U-62066E), a kappa-opioid receptor agonist, on neuroendocrine function in man. Br J Pharmacol. 1997;120(5):781–4.
19. Ben-Jonathan N, Arbogast LA, Hyde JF. Neuroendocrine [corrected] regulation of prolactin release. Prog Neurobiol. 1989;33(5–6):399–447.
20. Verhoest PR, Sawant-Basak A, Parikh V, Hayward M, Kauffman GW, Paradis V, McHardy SF, McLean S, Grimwood S, Schmidt AW, Vanase-Frawley M, Freeman J, Van Deusen J, Cox L, Wong D, Liras S. Design and discovery of a selective small molecule kappa opioid antagonist (2-methyl-N-((2'-(pyrrolidin-1-ylsulfonyl)biphenyl-4-yl)methyl)propan-1-amine, PF-4455242). J Med Chem. 2011. doi:10.1021/jm2006035.
21. Kalvass JC, Maurer TS, Pollack GM. Use of plasma and brain unbound fractions to assess the extent of brain distribution of 34 drugs: comparison of unbound concentration ratios to *in vivo* p-glycoprotein efflux ratios. Drug Metab Dispos. 2007;35(4):660–6.
22. CSR B1071001. A phase I, placebo-controlled, crossover study to evaluate the safety, tolerability and pharmacokinetics of PF 04455242 after first-time administration of single ascending doses to healthy adult subjects. 17 November 2009. Data on file.
23. CSR B1071002. A phase I, randomized, placebo controlled, multiple dose study to determine safety, tolerability and pharmacokinetics of PF-04455242 in healthy adult subjects. 10 August 2010. Data on file.
24. CSR B1071004. A phase I, randomized, placebo controlled proof of mechanism study to determine efficacy of PF-04455242 in blocking spiradoline (PF-00345768) stimulated prolactin release in healthy male adult subjects. 18 June 2010. Data on file.
25. Hong Y, Mager DE, Blum RA, Jusko WJ. Population pharmacokinetic/pharmacodynamic modeling of systemic corticosteroid inhibition of whole blood lymphocytes: modeling interoccasion pharmacodynamic variability. Pharm Res. 2007;24(6):1088–97.
26. Kalvass JC, Olson ER, Cassidy MP, Selley DE, Pollack GM. Pharmacokinetics and pharmacodynamics of seven opioids in P-glycoprotein-competent mice: assessment of unbound brain $EC_{50}$, u and correlation of *in vitro*, preclinical, and clinical data. J Pharmacol Exp Ther. 2007;323(1):346–55.
27. Mager DE, Lin SX, Blum RA, Lates CD, Jusko WJ. Dose equivalency evaluation of major corticosteroids: pharmacokinetics and cell trafficking and cortisol dynamics. J Clin Pharmacol. 2003;43 (11):1216–27.
28. Shimada S, Nakajima Y, Yamamoto K, Sawada Y, Iga T. Comparative pharmacodynamics of eight calcium channel blocking agents in Japanese essential hypertensive patients. Biol Pharm Bull. 1996;19(3):430–7.
29. Beal SL, Sheiner LB. NONMEM user's guides. San Francisco: NONMEM Project Group, University of California; 1992.
30. FDA's Guidance for Industry: Population Pharmacokinetics. February 1999.
31. Yano Y, Beal SL, Sheiner LB. Evaluating pharmacokinetic/pharmacodynamic models using the posterior predictive check. J Pharmacokinet Pharmacodyn. 2001;28(2):171–92.
32. Koch Y, Chow YF, Meites J. Metabolic clearance and secretion rates of prolactin in the rat. Endocrinology. 1971;89(5):1303–8.
33. Molitch ME, Raiti S, Baumann G, Belknap S, Reichlin S. Pharmacokinetic studies of highly purified human prolactin in normal human subjects. J Clin Endocrinol Metab. 1987;65 (2):299–304.
34. Pfeiffer A, Knepel W, Braun S, Meyer HD, Lohmann H, Brantl V. Effects of a kappa-opioid agonist on adrenocorticotropic and diuretic function in man. Horm Metab Res. 1986;18(12):842–8.
35. Rimoy GH, Bhaskar NK, Wright DM, Rubin PC. Mechanism of diuretic action of spiradoline (U-62066E)—a kappa opioid receptor agonist in the human. Br J Clin Pharmacol. 1991;32 (5):611–5.
36. Meibohm B, Derendorf H. Pharmacokinetic/pharmacodynamic studies in drug product development. J Pharm Sci. 2002;91 (1):18–31.